Journal of Photochemistry & Photobiology, B: Biology 153 (2015) 206–214

Contents lists available at ScienceDirect

Journal of Photochemistry & Photobiology, B: Biology

journal homepage: www.elsevier.com/locate/jpb

Antimony(III) complexes with 2-amino-4,6-dimethoxypyrimidines: Synthesis, characterization and biological evaluation

Turgay Tunç [a], Mehmet Sayım Karacan [b,*], Hatice Ertabaklar [c], Musa Sarı [d], Nurcan Karacan [b], Orhan Büyükgüngör [e]

[a] Ahi Evran University, Faculty of Engineering-Architecture, Departmant of Chemistry and Process Engineering, Kirsehir, Turkey
[b] Gazi University, Science Faculty, Chemistry Department, Ankara, Turkey
[c] Department of Physics, Faculty of Science and Arts, Ondokuz Mayıs University, Samsun, Turkey
[d] Department of Physics Education, Gazi University, Ankara, Turkey
[e] Adnan Menderes University, Medicine Faculty, Parasitology Department, Aydin, Turkey

ARTICLE INFO

Article history:
Received 28 June 2015
Received in revised form 28 August 2015
Accepted 21 September 2015
Available online 25 September 2015

Keywords:
Antimony(III) complexes
Antileishmanial activity
Glutathione reductase inhibition

ABSTRACT

Novel pyrimidine compound bearing disulfide bridge, 5,5′-disulfanediylbis(2-amino-4,6-dimetoxypyrimidine) (**3**) was synthesized by reduction of 2-amino-4,6-dimethoxy-5-thiocyanatopyrimidine for the first time, and its structure was confirmed by X-ray crystallographic analysis. Novel binuclear antimony(III) compound of (**3**), {Sb[5,5′-disulfanediylbis(2-amino-4,6-dimetoxypyrimidine)]Cl_3}$_2$ (**4**) and mononuclear antimony(III) compounds, SbL_2Cl_3, [L: 2-amino-5-thiol-4,6-dimethoxy pyrimidine (**2**) and 2-amino-5-(1H-tetrazol-5-ylthio)-4,6-dimethoxypyrimidine (**6**)] were synthesized and characterized with the help of elemental analysis, molecular conductivity, FT-IR, ^{1}H-NMR and LC–MS techniques. The geometrical structures optimized by a DFT/B3LYP/LANL2DZ method of the compounds, indicated that monomeric compounds have square pyramidal shape. Both antileishmanial activity against *Leishmania tropica* promastigote and glutathione reductase inhibitory activity were determined in vitro. The results showed that (**3**) has the best biological activity.

1. Introduction

Pyrimidines present a wide range of biological activities [1], as antifolate [2], antimicrobial [3,4], antifungal [5], anti-rubella [6], anti-HIV [7], antiviral [8], anti-inflammatory [9], antitumor [10,11], antimalarial [12,13] and antileishmanial [14–20] agents. On the other hands, tetrazoles exhibit appreciable biological activity [21], including glutathione reductase inhibitory activity [22] and antileishmanial activity against *Leishmania braziliensis* promastigotes [23].

Antimony-based compounds have been found to have several therapeutic effects, including antileishmaniasis, which were used in the treatment of leishmaniasis since ancient times [24–27], anthelminthic [28,29], antitrypanosomal [30], antimicrobial [31] and anticancer [32,33] agents. Glutathione reductase-targeting compounds are approved of new candidates as antimalarial and anticancer drugs [34,35]. We have recently reported that antimony(III) compounds exhibit good glutathione reductase inhibitory activities [36,37].

As a result of a virtual screening study, diphenylsulfanes were proposed as antiprotozoal drugs and trypanothione reductase inhibitors [38]. On the basis of previous virtual screening, we planned to obtain new antimony(III) compounds containing sulfide bridge, pyrimidine, and/or tetrazole groups to develop novel multitarget-directed drugs. As part of our ongoing works, in this study, three antimony(III) compounds, dimeric [Sb(5,5′-disulfanediylbis(2-amino-4,6-dimetoxypyrimidine))Cl_3]$_2$, and monomeric Sb(2-amino-5-thiol-4,6-dimethoxypyrimidine)$_2Cl_3$ **(4)** and (2-amino-5-(1H-tetrazol-5-ylthio)-4,6-dimethoxypyrimidine)$_2Cl_3$ **(6)** were synthesized and identified by using IR, NMR, LCMR, conductivity and calculation with a DFT/B3LYP/LANL2DZ method. In addition, 5,5′-disulfanediylbis(2-amino-4,6-dimetoxypyrimidine) was obtained by reduction of 2-amino-4,6-dimethoxy-5-thiocyanatopyrimidine for the first time and its structure was identified by X-ray crystallographic analysis. Additionally, their glutathione reductase activity and antileishmanial activity were determined.

2. Materials and Methods

2.1. Materials and Instrumentation

Glutathione reductase (GR) from baker's yeast (*Saccharomyces cerevisiae*) and other chemicals were purchased from Sigma-Aldrich (USA). Elemental analyses for C, H and N were carried out with a LECO CHNS-932 auto elemental analyser. Melting points were measured using an Electrothermal 9100 apparatus (Thermo Fisher Scientific, UK). The molecular conductivities of the complexes were measured

* Corresponding author.
E-mail address: mkaracan@gazi.edu.tr (M.S. Karacan).

http://dx.doi.org/10.1016/j.jphotobiol.2015.09.022
1011-1344/

with WTW Cond 330i. Infrared spectra from 4000 to 400 cm^{-1} were obtained in KBr pellets with a Mattson 1000 FT-IR spectrometer. NMR spectra were recorded in DMSO-d_6 with a Bruker Ultrashield 300 MHz spectrometer. Mass spectra were recorded with a Water Micromass ZQ spectrometer, coupled to a Waters 2695 separation module, LC–MS spectrometers in methanol/ acetonitrile mixture.

2.2. Preparation of Compounds

2-amino-4,6-dimethoxy-5-thiocyanatopyrimidine **(1)** and 2-amino-5-(1H-tetrazole-5-ylthio)-4,6-dimethoxypyrimidine **(5)** were synthesized according to reported procedures [39]. All newly prepared compounds were synthesized according to the procedure (Fig. 1).

2.2.1. Synthesis of bis(2-amino-5-thiol-4,6-dimethoxypyrimidine) trichloroantimony(III) (2)

0.52 g 2-amino-4,6-dimethoxy-5-thiocyanatopyrimidine **(1)** was dissolved in acetonitrile and 0.28 g antimony(III) chloride was added to the solution in the mole ratio of 2:1. The mixture was refluxed for 4 days at 82 °C. Evolution of reddish gas was observed after 2 h. The reaction mixture was cooled to room temperature and allowed to stand for overnight at room temperature. The obtained white products were filtered off and dried in air (0.12 g, yield: 15%, m.p. ˃400 °C). Calc. for $C_{12}H_{18}Cl_3N_6O_4S_2Sb$: C: 25.28, H: 3.43, N: 13.61, S: 10.38. Found: C: 24.37, H: 3.74, N: 13.82, S: 11.03. LC–MS [m/z]: 603.09 $[MH]^+$ (calc. $[M]^+$: 602.66); ^{1}H-NMR (DMSO-d_6, 300 MHz): 10.65 (s, 1H, SH), 7.00 (2H, NH_2), 3.66 (s, 6H, CH_3). ^{13}C-NMR (DMSO-d_6, 100 MHz,): 171.67, 170.44, 163.47, 71.83, 55.27; FTIR (KBr ν/cm^{-1}): 3466(m), 2941(m), 1653(m), 1591(m).

2.2.2. Synthesis of 5-5′-disulfanediylbis(2-amino-4,6-dimetoxypyrimidine) (3)

0.35 g of 2-amino-4,6-dimethoxy-5-thiocyanatopyrimidine **(1)** and 0.025 g of triphenylantimony(III) were dissolved in methanol (15 mL). pH was adjusted to ~10 with addition of trimethylamine. The mixture was stirred for 24 h at 60 °C. Yellow colored product was filtered off and dried at room temperature (0.40 g, yield 43%, m.p. 277–278 °C). Single crystals for X-ray diffraction were obtained by slow evaporation

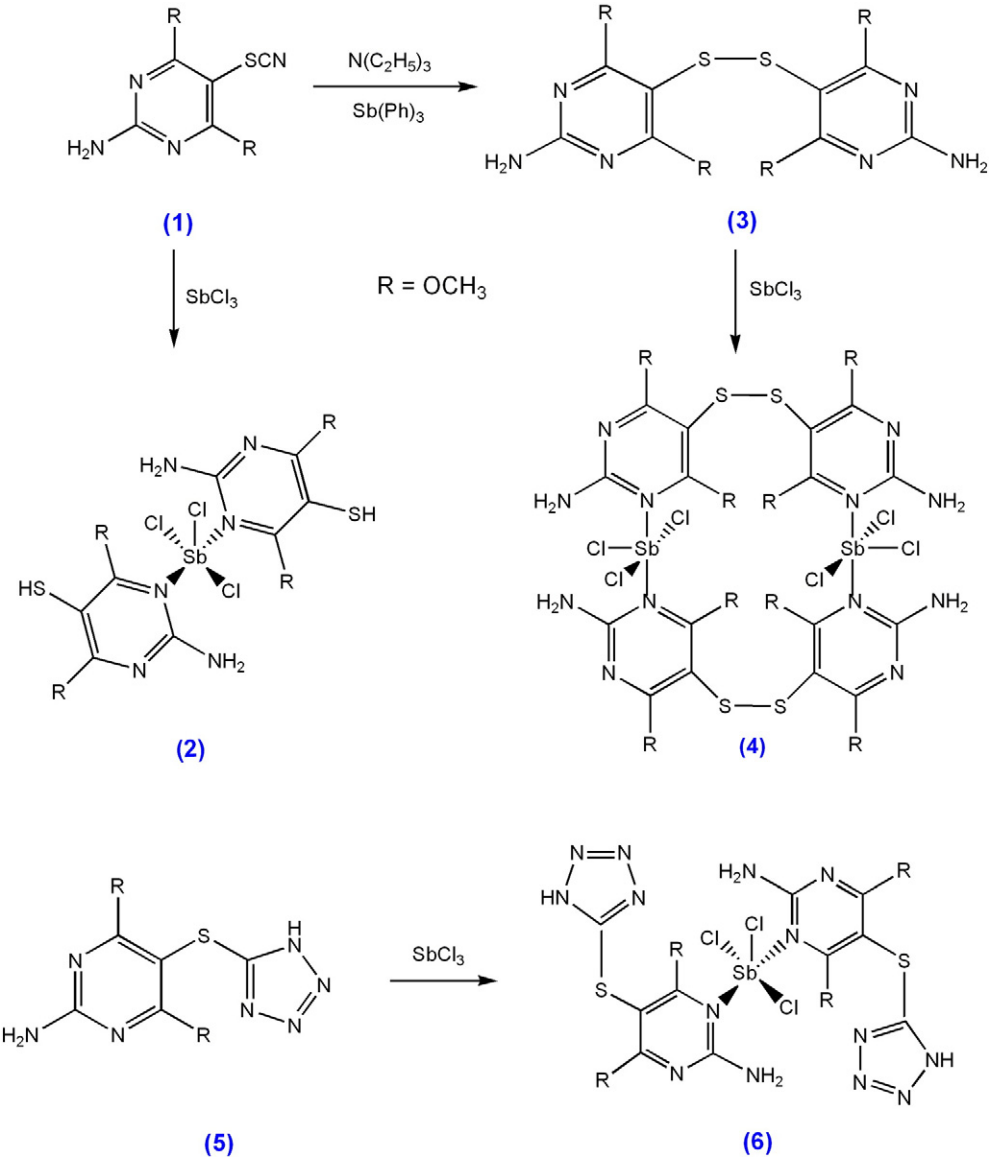

Fig. 1. Schematic diagram of the synthetic pathway of our compounds.

from a 1:9 acetone/DMSO solution. LC–MS [m/z]: 373.07 $[MH]^+$ (calc. $[M]^+$: 372.42); ^{1}H-NMR (300 MHz, DMSO-d_6, δ in ppm): 6.90 (s, 2H, NH_2); 3,70 (s, 6H, OCH_3). ^{13}C-NMR (100 MHz, DMSO-d_6): 171.25, 162.50, 86.89, 54.22; FTIR (KBr, ν/cm^{-1}): 3466(m), 2941(m), 1639(m), 1553(m).

2.2.3. Synthesis of bis[2-amino-5-5′-disulfanediylbis (4,6-dimetoxypyrimidine)trichloroantimony(III)] ***(4)***

0.3 g of **(3)** was dissolved in DMSO (15 mL) and 0.19 g of antimony(III) chloride was added to the solution in the mole ratio of 1:1. pH was adjusted to 5 with conc. HCl. The mixture was refluxed for 10 days at 180 °C, than it was evaporated to 1/3 of its initial volume. After refluxing, the reaction mixture was cooled to room temperature. After adding 10 mL of water, resulting product was allowed to stand for overnight in a refrigerator. Pink solid were filtered off and dried in air. (0.085 g, yield: 17%, m.p. >400 °C). Calc. for $C_{24}H_{32}Cl_6N_{12}O_8S_4Sb_2$: C: 25.37, H: 3.11, N: 13.65, S: 10.42. Found: C: 26.21, H: 3.18, N: 12.79, S: 10.13. LC–MS [m/z]: 1202.33 $[MH]^+$ (calc. $[M]^+$: 1201.08), ^{1}H-NMR (300 MHz, DMSO-d_6,): 6.70 (s, 2H, NH_2), 3.70 and 3.35 (s, 6H, OCH_3). FTIR (KBr/cm^{-1}): 3460(m), 2935(m), 1644(m), 1584(m).

2.2.4. Synthesis of bis(2-amino-5-(1H-tetrazol-5-ylthio)-4,6-dimethoxypyrimidine) trichloroantimony(III) ***(6)***

0.3 g of 2-amino-5-(1H-tetrazol-5-ylthio)-4,6-dimethoxypyrimidine **(5)** was dissolved in methanol (10 mL) and 0.13 g of antimony(III) chloride was added to the solution in the mole ratio of 2:1. pH was adjusted to 5 with conc. HCl. The mixture was refluxed for 2 days at 60 °C. The reaction mixture was cooled to room temperature and allowed to stand for overnight at room temperature. The obtained colorless products were filtered off and dried in air (0.2 g, yield: 46%, m.p. ˃400 °C). Calc. for $C_{14}H_{18}Cl_3N_{14}O_4S_2Sb$: C: 22.77, H: 2.46, N: 26.55, S: 8.68. Found: C: 23.07, H: 2.79, N: 26.11, S: 9.04. LC–MS [m/z]: 779.03 $[M + CH_3CN]^+$ (calc. $[M]^+$: 738.63); ^{1}H-NMR (DMSO-d_6, 300 MHz): 15.60 (s, 1H, NH), 7.20 (s, 2H, NH_2), 3.80 (6H, CH_3). ^{13}C-NMR (100 MHz, DMSO-d_6): 172.24, 171.11, 162.84, 156.33, 75.37, 54.92. FTIR (KBr, ν/cm^{-1}): 3431(m), 3332(m), 2922(m), 1701(m), 1649(m), 1547(m).

2.3. Glutathione Reductase Inhibition Assay

Glutathione reductase from baker's yeast (*S. cerevisiae*) activity was measured with a standard protocol [40]. All studies were carried out at physiological substrate concentrations in an assay buffer (20.5 mM KH_2PO_4, 26.5 mM K_2HPO_4, 200 mM KCl, 1 mM EDTA, pH 6.9 at 25 °C). The assay mixture (1.0 mL) contained 100 nmol of NADPH and 1 U of GR. In order to exclude nonspecific NADPH oxidation, the absorbance at 340 nm was monitored for 2 min. The reaction was started by adding 1 mM of GSSG. Oxidation of NADPH was monitored continuously by recording the decrease in absorbance at 340 nm. Inhibition of GR was studied in the presence of varying inhibitor concentrations; 1 mM stock solutions of the compounds were prepared by dissolving in minimum amount of dimethyl sulfoxide (DMSO) and diluting with water. All other compounds were dissolved in an assay buffer. The residual enzyme activity in the presence of inhibitor was determined relative to a control containing solvent but no inhibitor. From these data, IC_{50} values were determined graphically. For determining K_M values, the concentration of NADPH was kept constant at 5 mM, but concentration of GSSG was systematically varied from 1 mM to 5 mM.

2.4. In Vitro Leishmanicidal Activity Assay

The method described by Östan et al. was used for determination of antileishmanial activity of the compounds [41]. Promastigotes of

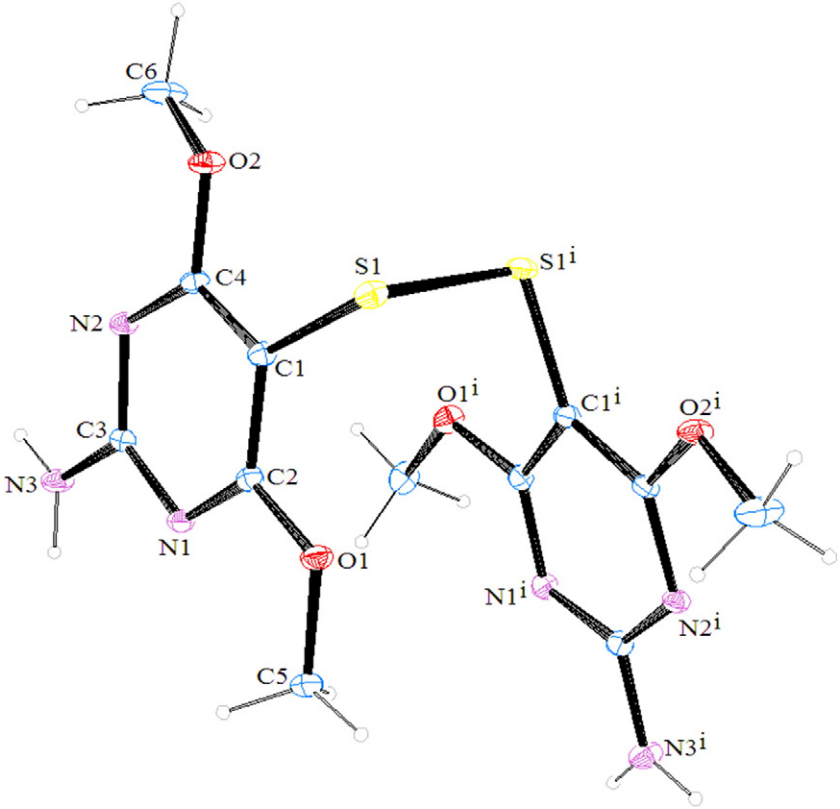

Fig. 2. An ORTEP drawing of **(3)** with the atom-numbering scheme. Displacement ellipsoids are drawn at the 40% probability level.

Table 1
Crystal data and structure refinement details for the compound **(3)**.

Chemical formula	C12H16N6O4S2
Formula weight	372.45
Temperature (K)	296(2)
Wavelength (Å)	0.71073
Crystal system, space group	Orthorhombic, Pbcn
Unit cell dimensions: (Å, °)	
a	7.5362(5)
b	14.6866(13)
c	14.7930(10)
Volume ($Å^3$)	1637.3(2)
Z	4
Absorbtion coefficient (mm^{-1})	0.357
Calculated density (Mg m^{-3})	1.511
F(000)	776
Crystal size (mm)	0.650 × 0.317 × 0.080
Theta range for data collection(°)	2.75–26.49
Limiting indices	−9 ≤ h ≤ 9, −18 ≤ k ≤ 18, −18 ≤ l ≤ 16
Reflections collected	9233
Independent reflections	1709
Number of reflections used	1261
Number of parameters	109
Max. and min. transmissions	0.873, 0.972
Refinement method	Ful-matrix least-squares on F2
Final R indices [I ≥ 2σ(I)]	R1 = 0.0417, wR2 = 0.0920
R indices (all data)	R1 = 0.0669,wR2 = 0.01003
Goodness of fit on F^2	0.993
Largest difference in peak and hole (e $Å^{-3}$)	0.231 and −0.199

Leishmania tropica were isolated from a patient from Aydin, Turkey using the NNN medium. Promastigotes transferred to the RPMI 1640 medium supplemented with 15% fetal calf serum for mass cultivation. Compounds were diluted with DMSO transferred to the culture plates to obtain final concentrations of 250, 125, 62.5, 31.2, 15.6, 7.8 μg/mL. After 1 h at 37 °C, 150 μL of the culture medium complemented with 1×10^6 parasites/mL, from a logarithmic phase culture, were added. DMSO and glucantime were used as drug carrier control and positive control (20 μg/mL), respectively. All plates were incubated at 26 °C. After 24, 48 and 72 h; viable *L. tropica* promastigotes were identified and counted microscopically with a hemocytometer on the basis of their aspect and motility. After incubation samples of each well were subcultured in a fresh medium for another 48 h without drugs. All tests were carried out in triplicate. All microscopic examinations were performed blindly by two investigators. MLC (The minimum lethal concentration) was determined to be the lowest concentration of drugs at which no motile cells were found. Growth inhibition (GI) % as calculated with respect to the growth control is as follows: %GI = $(1\text{-}GR_{extract}/GR_{control})X100$.

2.5. Single-crystal Structure Determination

Crystallographic data of **(3)** was recorded on a Stoe IPDS II CCD X-ray diffractometer employing plane graphite monochromatized with MoK_α

Table 2
Selected bond distances and angles for the compound **(3)**.

C1–S1	1.747(2)	C3–N2	1.345(3)
C2–O1	1.340(2)	C3–N3	1.344(3)
C4–O2	1.342(2)	C4–N2	1.327(3)
C5–O1	1.432(3)	S1–$S1^i$	2.0824(14)
C6–O2	1.426(3)	$C1^i$–$S1^i$	1.747(2)
C2–N1	1.315(3)		
N1–C2–O1	118.97(18)	N2–C4–O2	118.84(17)
N2–C3–N1	127.11(19)	C2–O1–C5	117.82(18)
N3–C3–N1	116.27(18)	C4–O2–C6	118.68(16)
N3–C3–N2	116.62(10)	C1–S1–$S1^i$	102.63(8)

Symmetri code: (i) −x, −y + 1, −z

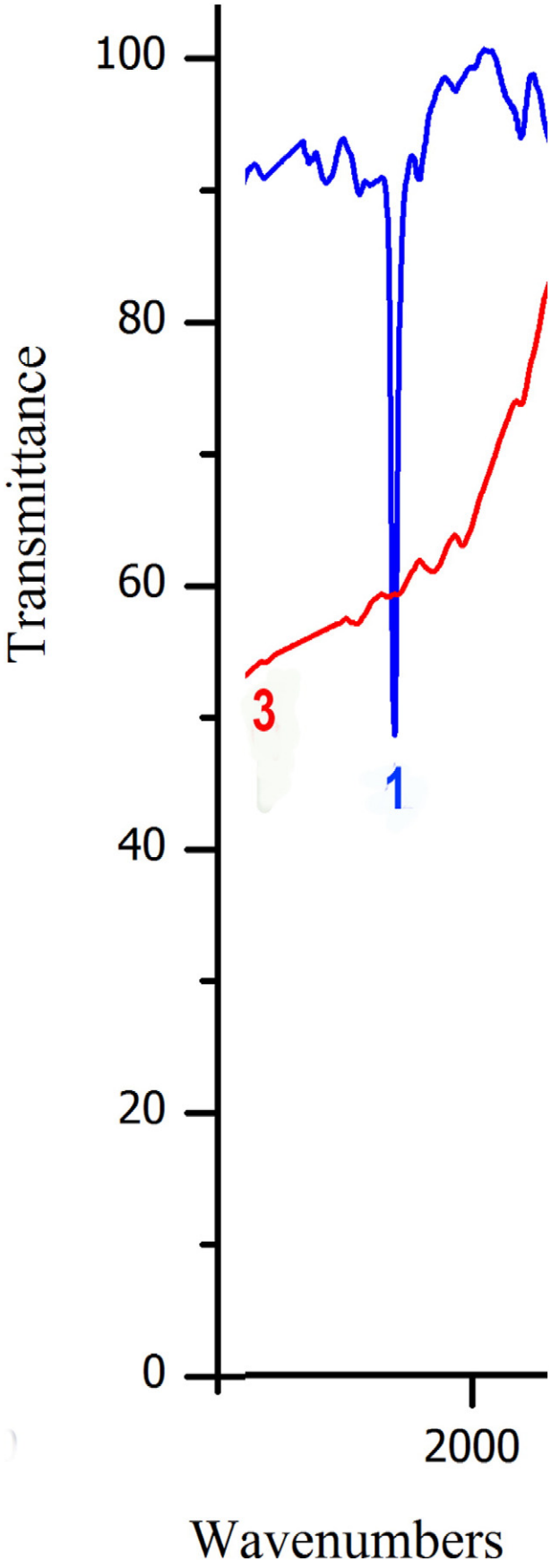

Fig. 3. Part of IR spectra of the **(1)** and **(3)** between 2500 and 1900 cm^{-1}.

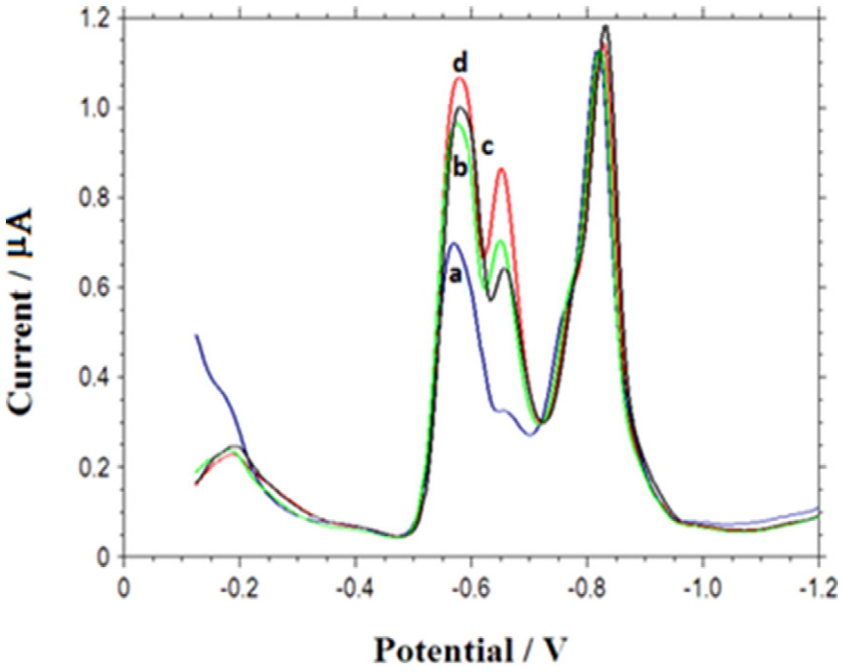

Fig. 4. Square wave voltammograms of compound **(2)** and Sb(III) additions at HMDE electrode vs Ag/AgCl (phosphate buffer in aqueous solution pH: 6.5).

radiation (λ = 0.71073 Å), using ω-2θ scan mode. The structures were solved by the direct methods and refined by full-matrix least-squares techniques on F^2 using the solution program SHELXS-97 and refined using SHELXL-97 [42]. The empirical absorption corrections were applied by the integration method via X-RED software [43]. The hydrogen atoms were included in their idealized positions and refined isotropically at distances of 0.95 Å (CH) from the parent C atoms; a riding model was used during the refinement process. An ORTEP drawing [44] of the molecule with 40% probability displacement thermal ellipsoids and atom-labeling schemes are shown in Fig. 2. The crystal and instrumental parameters used in the unit-cell determination and data collection are summarized in Table 1.

2.6. Computational Method

Full geometry optimizations were carried out using the density functional theory (DFT) method at the B3LYP level and LanL2DZ basis set. The vibrational frequency calculations were performed to ensure that the optimized geometries represent the local minima and that there are only positive eigenvalues. All calculations were performed with the GAUSSIAN03 program package [45] with the aid of the GaussView visualization program.

3. Results and Discussion

3.1. Crystal Structures of (3)

The crystal structures of **(3)** with the atom labeling is shown in Fig. 2. The details of the crystal structure solutions are summarized in Table 1 and the selected bond lengths and angles are listed in Table 2. The compound, $C_{12}H_{16}N_6O_4S_2$, crystallizes in the Orthorhombic, Pbcn space group. The compound has a center of symmetry and the S1 atom lies on the center of the mean planes. The linkage of the –S–S-bond between two aminopyrimidine rings and the dihedral angle between two aminopyrimidine rings is 90.79(19) Å. In the structure, the two aminopyrimidine rings are in axial position. The symmetric unit, the S1–S1i, C1–S1 and C1–S1i bond distances lie within a range of 2.0824(14) Å and 1.747(2) Å, respectively (Table 2). All bond distances and angles for the compound are consistent with those found in related compounds [46–48].

3.2. Synthesis and Formulation of the Compounds

New antimony(III) complex **(2)** was synthesized through a one-step synthesis by reacting antimony(III) chloride with **(1)**. In this reaction, the SCN group on pyrimidine ring is reduced to SH. As seen in part of IR spectra (Fig. 3), ν_{SCN} stretching vibration of **(1)** at 2154 cm^{-1} disappears, and a broad singlet peak at 10.65 ppm corresponding to labile proton of SH group was appeared [49] in the ^{1}H-NMR spectrum of **(2),** given in Fig. S1 in supplementary material. The mass spectrum of **(2),** given in Fig. S2, shows a peak at m/z 603.09 $[MH]^+$ corresponding to SbL_2Cl_3 molecular formula. We wondered whether antimony(III) atom was oxidized simultaneously. For this reason, square wave voltammograms of **(2)** and Sb(III) additions at HMDE electrode vs Ag/AgCl (phosphate buffer in aqueous solution pH: 6.5) were recorded and given in Fig. 4. As shown in Fig. 4, two reduction peaks for **(2)** were obtained at about −0.6 V and −0.8 V. Increasing of peak height at −0.6 V with addition of Sb(III) solution to the medium indicated that this peak can be assigned to reduction of Sb(III) to Sb(0). Chronoamperometric measurements also show that transferred electron number in this electrochemical reduction was 3. The other peak showing no change is adsorption peak of the **(2)**.

On the other hand, if triphenylantimony(III) is used instead of antimony(III) chloride bidentate ligand **(3)** was obtained in the presence of trimethylamine. In this reaction, thiocyanate group on pyrimidine ring was reduced and resulting intermediate was dimerised. In the second trial, same reaction without triphenylantimony(III) also gave **(3)** but a much longer time. This result showed that triphenylantimony(III) acted as a catalyst. In the literature, following reactions were reported for electrochemical reduction of aryl thiocyanates [50].

$$ArSCN + 2\acute{e} \rightarrow ArS^- + CN^-$$
$$ArSCN + ArS^- \rightarrow ArSSAr + CN^-$$

A peak at m/z 373.07 $[MH]^+$ of the mass spectrum of **(3),** given in Fig. S3, confirms the structure of **(3)** containing AsSSAr moiety.

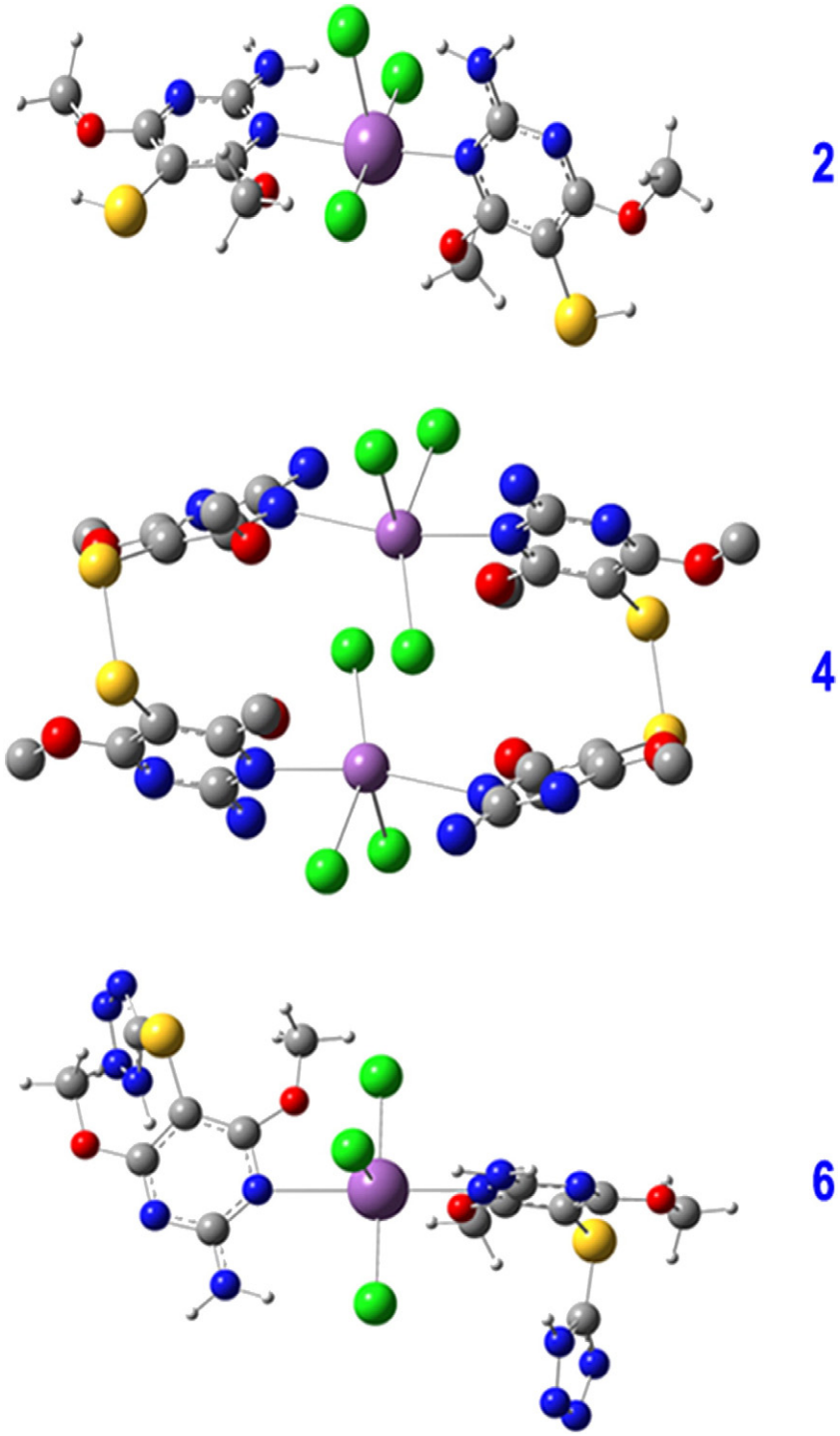

Fig. 5. Optimized structures calculated with B3LYP/LANL2DZ level.

The reaction of ligand **(3)** with antimony(III) chloride gave the pink product **(4)** in poor yield and in a long time. The mass spectrum of **(4),** given in Fig. S4, shows a peak at m/z 1202.34 $[MH]^+$ corresponding to $Sb_2L_2Cl_6$ molecular formula. The mass fragmentation at 631.48 corresponding to half of M with solvent fragment $[1/2\ M + CH_3CN]^+$ supports the molecular formula.

The reaction of ligand **(5)** with antimony(III) chloride gave the colorless product **(6)**. The mass spectrum of **(5)**, given in Fig. S5, shows a peak at m/z 779.03 $[M + CH_3CN]^+$ corresponding to SbL_2Cl_3 molecular formula.

The molar conductance values in DMF solution of 1×10^{-3} M of the complexes at 25 °C were found to be in the range 7.85–18.30 Ω^{-1} mol^{-1} cm^2. The relatively low values indicate that all complexes are non-electrolytes. According to obtained data, ligands **(1)** and **(5)** act as neutral and monodentate ligands with one N donor atom on pyrimidine ring, however, ligand **(3)** acts as a bidentate ligand with one N donor atom on two different pyrimidine rings and gave dinuclear complex **(4)**.

Geometries of all complexes were optimized using a DFT/B3LYP/LANL2DZ method/basis set to find the most stable structures.

Table 3
NMR chemical shifts values of the compounds.

Assignment	Ligands			Complexes		
	1	3	5	2	4	6
^{1}H-NMR						
OCH_3	3.92 s	3.70 s	3.82 s	3.66 s	1.40 s	3.80 s
NH_2	7.37 s	6.90 s	7.22 s	7.00 s	6.70 s	7.20 s
NH	–	–	15.98 s	–	–	15.60 s
SH	–	–	–	10.65 s	–	–
^{13}C-NMR						
O**C**H_3	55.12	54.22	54.64	55.27		54.92
C–SCN	71.84		–	71.83		–
S–**C** (prmd)		86.89	74.90	–		75.37
S–**C** (przl)			155.38	–		156.33
S**C**N	112.57			–		
C–NH_2	163.50	162.50	163.47	163.47		162.84
C–OCH_3	170.56	171.25	171.32	170.44		171.11
				171.67		172.24

Calculation results, given in Fig. 5, show that the ground state optimized geometry of all complexes has square-pyramidal geometry. **(2)** and **(6)** have a plane with two N donor atoms and two Cl atoms in the trans arrangement, and one Cl atom above the plane (in apical position). Two equatorial Sb–Cl bonds are long (mean: 2.71 Å) and one apical Sb–Cl bond is short (Sb–Cl = 2.59 Å).

3.3. Spectral Analysis of the Complexes

^{1}H-NMR and ^{13}C-NMR spectra of the free ligand (**1**, **3**, and **5**) and their complexes (**2**, **4** and **6**) were given in Fig. S6–Fig. S14. The chemical shifts of the ligands and their antimony(III) complexes are listed in Table 3. Assignments of the carbon atoms in the ^{13}C-NMR spectrum of the complex **(4)** was not performed due to low solubility in DMSO-d_6 and poor resolution of the obtained spectrum. The NMR spectra of the complexes were evaluated by a comparative analysis with the spectra of free ligands. Results can be summarized as follows:

(a) The signal at 112.57 ppm, which belongs to the carbon atom of SCN group of **(1)**, is disappeared, as mentioned above a new signal appeared at 10.65 ppm, confirming the reduction of this group with complex **(2)** formation.
(b) No significant differences concerning the chemical shifts of NH_2 protons were observed with a complex formation, excluding the possible coordination of ligands to the antimony(III) through nitrogen of NH_2 groups.
(c) Proton signals of OCH_3 and NH_2 of the **(1)** were shifted upfield in comparison to that of **(3)**.
(d) Proton signals of OCH_3 with complex formation show no significant shifting, except for binuclear complex (**4**).
(e) Signals of the ring C atom bound to the OCH_3 group at about 170 ppm appear as two well-separated multiplets in the range between 170 and 172 ppm; this was attributed to having two different chemical environments with complex formation.

Table 4
Glutathione reductase inhibitory activity of the compounds.

Comp.	IC_{50} (μM)	K_i (μM)	Comp	IC_{50} (μM)	Ki (μM)
(1)	334.57 ± 10.41	162.01 ± 47.20	**(2)**	9.19 ± 0.30	1.79 ± 0.56
(3)	258.22 ± 8.48	122.70 ± 32.90	**(4)**	567.07 ± 75.01	43.4 ± 13.20
(5)	349.80 ± 12.01	158.68 ± 40.60	**(6)**	28.67 ± 3.40	27.9 ± 8.20

IR spectra of the complexes (**2**, **4**, and **6**) show the same spectral pattern. ν_{CN} and ν_{ring} stretching vibrations of the free pyrimidine ring at ~1561 cm^{-1} and ~994 cm^{-1} were shifted considerably towards higher

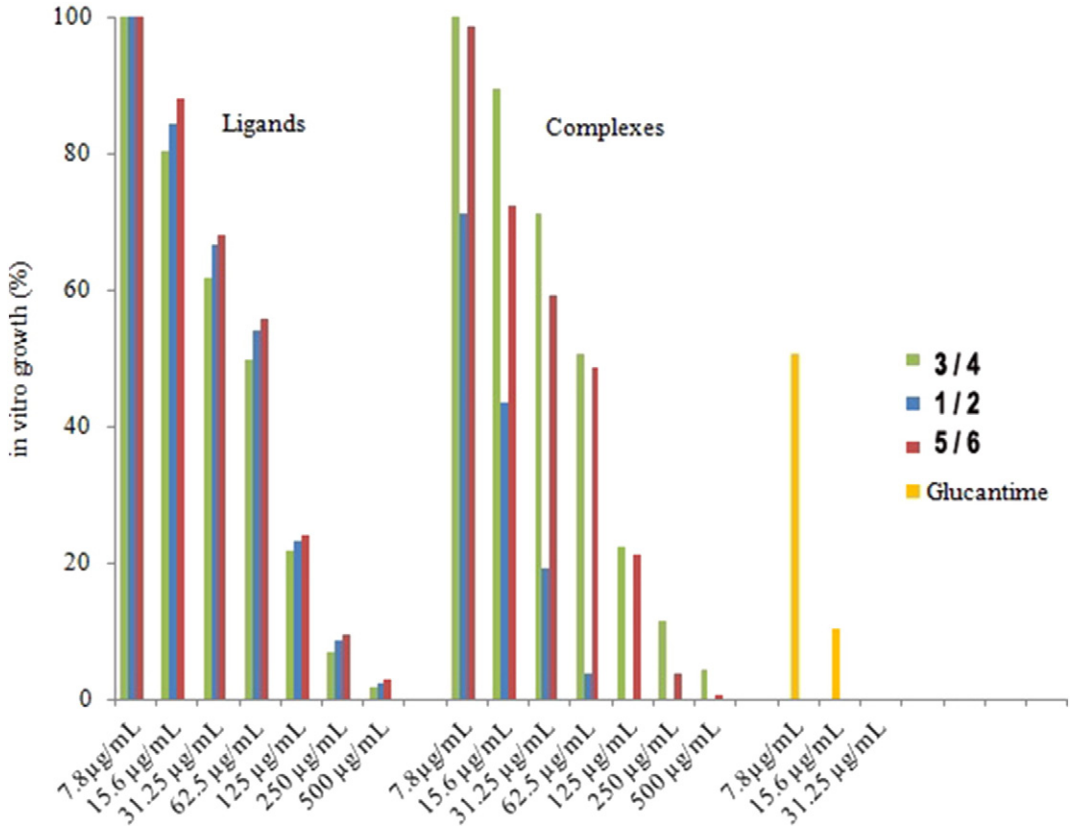

Fig. 6. Antileishmanial activity of the compounds.

frequency with complex formation, indicating that pyrimidine bonded to antimony through nitrogen donor atom [51]. ν_{NH2} stretching vibrations in complexes are not shifted considerably in comparison with that of free ligands, indicated that ligands do not coordinate with amine nitrogen atom.

3.4. In Vitro Antileishmanial Activity Evaluation

Antileishmanial activity data of the antimony(III) compounds and corresponding ligands, obtained against the pathogenic *L. tropica* promastigotes are pictorially presented in Fig. 6. Glucantime is used as a reference standard. Following results were achieved from the obtained data:

(a) Antimony(III) compounds show more antileishmanial activity than that of corresponding ligands.
(b) Compound **(3)**, bearing SS bridge and having four N donor atoms on pyrimidine ring, shows the best antileishmanial activity among the ligands. Compound **(1)**, having SCN substituents on pyrimidine ring shows the second highest activity. Contrary to expectations, tetrazole group on the pyrimidine ring does not increase the activity.
(c) Compound **(2)**, having SH group on the pyrimidine ring, exhibits the best antileishmanial activity (5.76% growth inhibition at 62.50 μg/mL) but lower activity than that of reference drug glucantime.
(d) Surprisingly, compound **(4)** shows the least activity among the antimony(III) compounds. We assume that increased molecular volume might be responsible for the decreasing antileishmanial activity.

3.5. Glutathione Reductase Inhibition

IC_{50} values were determined graphically from concentration − % activity curves (Fig. S15). Lineweaver–Burk graphs at fixed NADPH concentration at 5 mM and variable GSSG concentration in the range from 1 mM to 5 mM were drawn by using $1/V_{max}$ vs 1/[GSSG] values and K_i constant was calculated from these graphs (Fig. S16). Kinetic investigations indicate that all compounds exhibited competitive inhibition. Table 4 lists the IC_{50} and K_i values of all compounds. Compound **(2)** is identified as the most potent glutathione reductase inhibitor with IC_{50} and K_i value of 9.19 ± 0.30 μM and 1.79 ± 0.56 μM, respectively. Compound **(6)** behaved as the second strongest inhibitor. The antimony(III) complexes show more inhibitor activity than corresponding ligands. In addition, glutathione reductase inhibitory activity order of the compounds is similar to antileishmanial activity order.

4. Conclusions

Herein, we synthesized and characterized three new antimony(III) complexes bearing 2-amino-4,6-dimetoxypyrimidine derivatives as ligands. **(3)** acts as bidentate ligand and gives rise to binuclear antimony(III) complex **(4)**. Nevertheless, the remaining ligands (**1** and **2**) act as monodentate with one N donor atom on pyrimidine ring, and give two monomeric antimony(III) complexes (**2** and **6**). In addition, the glutathione reductase inhibitory activity and antileishmanial activity against the *L. tropica* promastigotes of all compounds were investigated. Results show that, monomeric antimony(III) compounds perform more antileishmanial and glutathione reductase inhibitory activity than that of corresponding ligands. However, binuclear antimony(III) complex is less effective than its ligand considering the increasing molecular volume decreases the biological activity. Compound **(2)** bearing SH group on the pyrimidine ring exhibits the best but lower antileishmanial activity compared to reference drug glucantime. Contrary to expectations, tetrazole group on the pyrimidine ring does not increase the activity. There is a strong correlation between in vitro antileishmanial activity against the parasite and inhibition of glutathione reductase by the antimony(III) complexes synthesized. It is well known that glutathione reductase is the nearest homologue to trypanothione reductase, which is a target for anti-trypanosomal as well as antileishmanial drugs [52]. In addition, Similarity between metabolic pathways of protozoa (*Leishmania*, *Trypanosoma*) and tumor cells also lead to a correlation between antitrypanosomal and antitumor activities [53]. Therefore, further studies to evaluate both anticancer and antimalarial activities of the compounds, especially for **(2)** should be done. As a matter of fact, in our experiments, we obtained that compound **(2)** has good plant glutathione reductase inhibitory activity.

Acknowledgments

This work has been supported in part by the Scientific and Technological Research Council of Turkey (TUBITAK Project no: 212T089). This work was partly founded by grants from Afyonkarahisar Kocatepe University, the Presidency of the Commission of Scientific Research Projects (BAPK-042.FENED.08). In addition, The authors thank to acknowledge the Faculty of Arts and Sciences, Ondokuz Mayıs University, Turkey, for the use of the Stoe IPDS-2 diffractometer purchased under grant F.279 of the University Research Fund.

Appendix A. Supplementary data

Supplementary data to this article can be found online at http://dx.doi.org/10.1016/j.jphotobiol.2015.09.022.

References

[1] G.W. Rewcastle, in: A.R. Katritzky, C.A. Ramsden, E.F.V. Scriven, R.J.K. Taylor (Eds.), Pyrimidines and Their Benzo Derivatives, Comprehensive Heterocyclic Chemistry III, 8, Elsevier, New York, NY, USA 2008, pp. 117–272.
[2] A. Gangjee, J. Yang, J.J. McGuire, R.L. Kisliuk, Synthesis and evaluation of a classical 2,4-diamino-5-substituted-furo[2,3-*d*]pyrimidine and a 2-amino-4-oxo-6-substituted-pyrrolo[2,3-*d*]pyrimidine as antifolates, Bioorg. Med. Chem. 14 (2006) 8590–8598.
[3] R. Aggarwal, E. Masan, P. Kaushik, D. Kaushik, C. Sharma, K.R. Aneja, Synthesis and biological evaluation of 7-trifluoromethylpyrazolo [1,5-a] pyrimidines as anti-inflammatory and antimicrobial agents, J. Fluor. Chem. 168 (2014) 16–24.
[4] R.P. Dhankar, A.M. Rahatgaonkar, M.S. Chorghade, A. Tiwari, Spectral and in vitro antimicrobial properties of 2-oxo-4-phenyl-6-styryl 1,2,3,4-tetrahydro-pyrimidine-5-carboxylic acid transition metal complexes, Spectrochim. Acta A 93 (2012) 348–353.
[5] K.M.H. Hilmy, M.M.A. Khalifa, M.A.A. Hawata, R.M.A.A. Keshk, A.A. El-Torgman, Synthesis of new pyrrolo[2,3-*d*]pyrimidine derivatives as antibacterial and antifungal agents, Eur. J. Med. Chem. 45 (2010) 5243–5250.
[6] L. Gupta, N. Sunduru, A. Verma, S. Srivastava, S. Gupta, N. Goyal, P.M.S. Chauhan, Synthesis and biological evaluation of new [1,2,4]triazino[5,6-*b*]indol-3-ylthio-1,3,5-triazines and [1,2,4]triazino[5,6-*b*]indol-3-ylthio-pyrimidines against *Leishmania donovani*, Eur. J. Med. Chem. 45 (2010) 2359–2365.
[7] X. Guo, Y. Li, L. Tao, Q. Wang, S. Wang, W. Hu, Z. Pan, Q. Yang, Y. Cui, Z. Ge, L. Dong, X. Yu, H. An, C. Song, J. Chang, Synthesis and anti-HIV-1 activity of 4-substituted-7-(2′-deoxy-2′-fluoro-4′-azido-β-D-ribofuranosyl)pyrrolo[2,3-*d*]pyrimidine analogues, Bioorg. Med. Chem. Lett. 21 (2011) 6770–6772.
[8] H.N. Hafez, H.A.R. Hussein, A.R.B.A. El-Gazzar, Synthesis of substituted thieno[2,3-*d*]pyrimidine-2,4-dithiones and their *S*-glycoside analogues as potential antiviral and antibacterial agents, Eur. J. Med. Chem. 45 (2010) 4026–4034.
[9] A.H. Abdelazeem, S.A. Abdelatef, M.T. El-Saadi, H.A. Omar, S.I. Khan, C.R. McCurdy, S.M. El-Moghazy, Novel pyrazolopyrimidine derivatives targeting COXs and iNOS enzymes; design, synthesis and biological evaluation as potential anti-inflammatory agents, Eur. J. Pharm. Sci. 62 (2014) 197-21.
[10] K.P. Shao, X.Y. Zhang, P.J. Chen, D.Q. Xue, P. He, L.Y. Ma, J.X. Zheng, Q.R. Zhang, H.M. Liu, Synthesis and biological evaluation of novel pyrimidine–benzimidazol hybrids as potential anticancer agents, Bioorg. Med. Chem. Lett. 24 (2014) 3877–3881.
[11] A.E. Kassab, E.M. Gedawy, Synthesis and anticancer activity of novel 2-pyridyl hexahyrocyclooctathieno[2,3-d]pyrimidine derivatives, Eur. J. Med. Chem. 63 (2013) 224–230.
[12] A. Agarwal, K. Srivastava, S.K. Puri, P.M.S. Chauhan, Antimalarial activity of 2,4,6-trisubstituted pyrimidines, Bioorg. Med. Chem. Lett. 15 (2005) 1881–1883.
[13] D. Kumar, S.I. Khan, B.L. Tekwani, P. Ponnan, D.S. Rawat, 4-Aminoquinoline – Pyrimidine hybrids: synthesis, antimalarial activity, heme binding and docking studies, Eur. J. Med. Chem. 89 (2015) 490–502.

[14] S.K. Patle, N. Kawathekar, M. Zaveri, P. Kamaria, Synthesis and evaluation of 2,4,6-trisubstituted pyrimidine derivatives as novel antileishmanial agents, Med. Chem. Res. 22 (2013) 1756–1761.
[15] D.H. Fleita, R.M. Mohareb, O.K. Sakka, Antitumor and antileishmanial evaluation of novel heterocycles derived from quinazoline scaffold: a molecular modeling approach, Med. Chem. Res. 22 (2013) 2207–2221.
[16] K. Ankur, J. Priyanka, B. Pankaj, Efficient computational analysis of 2-pyridyl pyrimidine derivetives for design of potent anti-leishmanial agents, Int. J. Pharm. Res. 4 (2012) 1439–1449.
[17] S.N. Suryawanshi, S. Kumar, R. Shivahare, S. Pandey, A. Tiwari, S. Gupta, Design, synthesis and biological evaluation of aryl pyrimidine derivatives as potential leishmanicidal agents, Bioorg. Med. Chem. Lett. 23 (2013) 5235–5238.
[18] G.S.G. de Carvalho, R.M.P. Dias, F.R. Pavan, C.Q.F. Leite, V.L. Silva, C.G. Diniz, D.T.S. de Paula, E.S. Coimbra, P. Retailleau, A.D. da Silva, Synthesis, cytotoxicity, antibacterial and antileishmanial activities of ımidazolidine and hexahydropyrimidine derivatives, Med. Chem. 9 (2013) 351–359.
[19] M. Iman, A. Davood, QSAR and QSTR study of pyrimidine derivatives to improve their therapeutic index as antileishmanial agents, Med. Chem. Res. 22 (2013) 5029–5035.
[20] D. Pathak, M. Yadav, N. Siddiquib, S. Kushawah, Antileishmanial agents: an updated review, Pharm. Chem. 3 (2011) 239–249.
[21] V.A. Ostrovskii, G.I. Koldobskii, R.E. Trifonov, Comprehensive Heterocyclic Chemistry III, 6, Tetrazoles; Elsevier, USA 2008, pp. 1–257.
[22] C. Biot, H. Bauer, R.H. Schirmer, E.D. Charvet, 5-substituted tetrazoles as bioisosteres of carboxylic acids. Bioisosterism and mechanistic studies on glutathione reductase inhibitors as antimalarials, J. Med. Chem. 47 (2004) 5972–5983.
[23] J.V. Faria, M.S. dos Santos, A.M.R. Bernardino, K.M. Becker, G.M.C. Machado, R.F. Rodrigues, M.M.C. Cavalheiro, L.L. Leon, Synthesis and activity of novel tetrazole compounds and their pyrazole-4-carbonitrile precursors against Leishmania spp. Bioorg. Med. Chem. Lett. 23 (2013) 6310–6312.
[24] Marcel Gielen, Edward R.T. Tiekin, Metallotherapeutic Drugs and Metal-Based Diagnostic Agents the Use of Metals in Medicine, John Wiley & Sons Ltd., 2005 443–444.
[25] F. Frezard, P.S. Martins, M.C.M. Barbosa, A.M. Pimenta, W.A. Ferreira, J.E. de Melo, J.B. Mangrum, C. Demicheli, New insights into the chemical structure and composition of the pentavalent antimonial drugs meglumine antimonate and sodium stibogluconate, J. Inorg. Biochem. 102 (2008) 656–665.
[26] A.J. Magill, D.R. Hill, T. Solomon, E.T. Ryan (Eds.), Hunter's Tropical Medicine and Emerging İnfectious Disease, Elsevier, London 2013, pp. 739–760.
[27] M.I. Khan, S. Gul, I. Hussain, M.A. Khan, M. Ashfaq, I.U. Rahman, F. Ullah, G.F. Durrani, I.B. Baloch, R. Naz, In vitro anti-leishmanial and anti-fungal effects of new Sb^{III} carboxylates, Org. Med. Chem. Lett. 1 (2) (2011) 1–7.
[28] T. Newlove, L.H. Guimarães, D.J. Morgan, L. Alcântara, M.J. Glesby, E.M. Carvalho, P.R. Machado, Antihelminthic therapy and antimony in cutaneous leishmaniasis: a randomized, double-blind, placebo-controlled trial in patients co-infected with helminths and *Leishmania braziliensis*, Am. J. Trop. Med. Hyg. 84 (2011) 551–555.
[29] Y.Z. Voloshin, O.A. Varzatskii, Y.N. Bubnov, Cage complexes of transition metals in biochemistry and medicine, Russ. Chem. B 56 (2007) 577–605.
[30] G.L. Parrilha, R.P. Dias, W.R. Rocha, I.C. Mendes, D. Benítez, J. Varela, H. Cerecetto, M. González, C.M.L. Melo, J.K.A.L. Neves, V.R.A. Pereira, H. Beraldo, 2-Acetylpyridine- and 2-benzoylpyridine-derived thiosemicarbazones and their antimony(III) complexes exhibit high anti-trypanosomal activity, Polyhedron 31 (2012) 614–621.
[31] N.C. Kasuga, K. Onodera, S. Nakano, K. Hayashi, K. Nomiya, Syntheses, crystal structures and antimicrobial activities of 6-coordinate antimony(III) complexes with tridentate 2-acetylpyridine thiosemicarbazone, bis(thiosemicarbazone) and semicarbazone ligands, J. Inorg. Biochem. 100 (2006) 1176–1186.
[32] I.I. Ozturk, C.N. Banti, M.J. Manos, A.J. Tasiopoulos, N. Kourkoumelis, K. Charalabopoulos, S.K. Hadjikakou, Synthesis, characterization and biological studies of new antimony(III) halide complexes with ω-thiocaprolactam, J. Inorg. Biochem. 109 (2012) 57–65.
[33] S.K. Hadjikakou, I.I. Ozturk, M.N. Xanthopoulou, P.C. Zachariadis, S. Zartilas, S. Karkabounas, N. Hadjiliadis, Synthesis, structural characterization and biological study of new organotin(iv), silver(i) and antimony(iii) complexes with thioamides, J. Inorg. Biochem. 102 (2008) 1007–1015.
[34] T. Müller, L. Johann, B. Jannack, M. Brückner, D.A. Lanfranchi, H. Bauer, C. Sanchez, V. Yardley, C. Deregnaucourt, J. Schrevel, M. Lanzer, R.H. Schirmer, E.D. Charvet, A glutathione reductase-catalyzed cascade of redox reactions to bioactivate potent antimalarial 1,4-naphthoquinones — a new strategy to combat malarial parasites, J. Am. Chem. Soc. 133 (2011) 11557–11571.
[35] F. Iribarne, M. Paulino, S. Aguilera, O. Tapia, Assaying phenothiazine derivatives as trypanothione reductase and glutathione reductase inhibitors by theoretical docking and molecular dynamics studies, J. Mol. Graph. Model. 28 (2009) 371–381.
[36] T. Tunç, Y. Koç, L. Açık, M.S. Karacan, N. Karacan, DNA cleavage, antimicrobial studies and a DFT-based QSAR study of new antimony(III) complexes as glutathione reductase inhibitor, Spectrochim. Acta Mol. Biomol. Spectrosc. 136 (2015) 1418–1427.
[37] M.S. Karacan, T. Tunç, H. Oruç, S. Mamaş, N. Karacan, A new method for screening glutathione reductase inhibitorsusing square wave voltammetry, Anal. Methods 7 (2015) 5142–5148.
[38] R.P. Pineiro, A. Burgos, D.C. Jones, L.C. Andrew, H. Rodriguez, M. Suarez, A.H. Fairlamb, D.S. Wishart, Development of a novel virtual screening cascade protocol to identify potential trypanothione reductase inhibitors, J. Med. Chem. 52 (2009) 1670–1680.
[39] A. Dişli, S. Mercan, S. Yavuz, Synthesis and antimicrobial activity of new pyrimidine derivatives incorporating 1*h*-tetrazol-5-ylthio moiety, J. Heterocycl. Chem. 50 (2013) 1446–1450.
[40] M.D. Maines, L.G. Costa, D.J. Reed, S. Sassa, I.G. Sipes, Current Protocols in Toxicology, John Wiley & Sons, Inc., Hoboken, NJ, 1999.
[41] I. Östan, H. Saglam, M.E. Limoncu, H. Ertabaklar, S.Ö. Toz, Y. Özbel, A. Özbilgin, In vitro and in vivo activities of *Haplophyllum myrtifolium* against *Leishmania tropica*, New Microbiol. 30 (2007) 439–445.
[42] G.M. Sheldrick, SHELXS97 and SHEXL97, Program for Crystal Structure Solution and Refinement, University of Göttingen, Germany, 1997.
[43] Stoe & Cie, X-AREA (Version 1.18) and X-RED32 (Version 1.04), Stoe & Cie, Darmstadt, Germany, 2002.
[44] L.J. Farrugia, J. Appl. Cryst. 30 (1997) 565.
[45] M.J. Frisch, et al., Gaussian 03 (Revision B.04), Gaussian, Inc., Pittsburgh PA, 2003.
[46] A.E. Ruiz, G.G. Gómez, E. Mijangos, A.P. Hueso, H.L. Sandoval, A.F. Parra, R. Contreras, N.B. Behrens, Coordination chemistry of a bis(benzimidazole) disulfide: eleven membered chelate ring in cobalt(II), zinc(II) and cadmium(II) halide compounds; oxidative disulfide cleavage when coordinated to nickel(II), Dalton Trans. 39 (2010) 6302–6309.
[47] J. Shang, W.M. Wang, Y.H. Li, H.B. Song, Z.M. Li, J.G. Wang, Synthesis, crystal structure, in vitro acetohydroxyacid synthase inhibition, in vivo herbicidal activity, and 3D-QSAR of new asymmetric aryl disulfides, J. Agric. Food Chem. 60 (2012) 8286–8293.
[48] G.J. Corban, C.D. Antoniadis, S.K. Hadjikakou, N. Kourkoumelis, V.Yu. Tyurin, A. Dolgano, E.R. Milaeva, M. Kubicki, P.V. Bernhardt, E.R.T. Tiekink, S. Skoulika, N. Hadjiliadis, Reactivity of di-iodine toward thiol: desulfuration reaction of 5-nitro-2-mercapto-benzimidazole upon reaction with di-iodine, Heteroat. Chem. 23 (2012) 498–511.
[49] A.M. Shakir, Synthesis and preliminary antimicrobial activities of new arylideneamino-1,3,4-thiadiazole-(thio/dithio)-acetamido cephalosporanic acids, Molecules 17 (2012) 1025–1038.
[50] A. Houmam, E.M. Hamed, I.W.J. Still, A unique autocatalytic process and evidence for a concerted-stepwise mechanism transition in the dissociative electron-transfer reduction of aryl thiocyanates, J. Am. Chem. Soc. 125 (2003) 7258–7265.
[51] A.H. Austin, S.T. Gregory, I.H. Nathan, Effects of hydrogen bonding on vibrational normal modes of pyrimidine, J. Phys. Chem. A 114 (2010) 6803–6810.
[52] A. Cavalli, M.L. Bolognesi, Neglected tropical diseases: multi-target-directed ligands in the search for novel lead candidates against *Trypanosoma* and *Leishmania*, J. Med. Chem. 52 (2009) 7339–7359.
[53] J. Benitez, L. Becco, I. Correia, S.M. Leal, H. Guiset, J.C. Pessoa, J. Lorenzo, S. Tanco, P. Escobar, V. Moreno, B. Garat, D. Gambino, Vanadium polypyridil compounds as potential antiparasitic and antitumoral agents: new achievements, J. Inorg. Biochem. 105 (2011) 303–312.